Quantum transport in disordered mesoscopic ferromagnetic films

Philip A. E. Jonkers,* Steven J. Pickering, and Hans De Raedt†
Rijksuniversiteit Groningen, 9747 AG Groningen, The Netherlands

Gen Tatara‡
Max Planck Institut fur Mikrostrukturphysik, Weinberg 2, 06120 Halle, Germany
and Graduate School of Science, Osaka University, Toyonaka, Osaka 560-0043, Japan
(Received 25 February 1999)

The effect of impurity and domain-wall scattering on the electrical conductivity of disordered mesoscopic magnetic thin films is studied by use of computer simulation. The results indicate a reduction of resistivity due to a domain wall, which is consistent with the explanation in terms of the dephasing caused by domain wall. [S0163-1829(99)03947-8]

The electrical transport properties of ferromagnetic metals have attracted much interest recently see, e.g., Refs. 1–3. In the present paper, we study the quantum transport in mesoscopic wires that contain a magnetic domain wall. The motion of the electrons passing through a wire that contains a magnetic domain wall is affected by various physical processes. As the electron approaches the domain wall it experiences a change in potential energy, leading to a reflection and hence to a reduction of the conductivity. However, unless the domain wall is unrealistically narrow (compared to the Fermi wavelength of the electrons) this reduction has been shown to be negligibly small[7] in the case of a spin-independent collision time. In the presence of a domain wall the spin of the electron will change as the electron passes through the wire. This rotation will lead to a mixing of spin-up and spin-down components. Assuming that the (Boltzmann) collision time is spin-dependent, this mixing then results in an increase of the resistivity, a scenario that has been proposed[8] to explain the experimental results on thin Co films at room temperature.[3] Spin dependent scattering is the essential ingredient in models for electron transport in magnetic materials that exhibit giant magnetoresistance (GMR).[9–12]

In disordered systems at low temperatures the quantum interference, which becomes important as a result of random spin-*in*dependent impurity scattering, also strongly influences the electron transport properties. Theoretical work[13] has shown that the domain wall suppresses the interference (and thus weak localization) due to impurity scattering, resulting in a decrease of the resistivity. Very recently there have been several experimental studies of a resistivity in a mesoscopic wire of ferromagnetic metals.[4–6] The results suggest a reduction of resistivity due to a domain wall, and interestingly the effect increases by lowering the temperature; below 50,[4] and 20 K (Ref. 6) respectively. This reduction might be related to the quantum decoherence caused by the wall. But other classical mechanisms of the reduction have also been proposed as well[4] and further studies are needed to clarify its origin. The purpose of the present paper is to study the interplay of the domain wall and spin-independent impurity scattering in more detail and to compare quantitatively the theoretical prediction of the Kubo-formula approach with first-principle quantum-mechanical calculations.

The geometry of the model system is shown in Fig. 1. The electrons are assumed to move in a two-dimensional metallic strip with a single magnetic domain wall. The Hamiltonian for this model reads

$$\mathcal{H}=\frac{1}{2m^*}(\mathbf{p}-e\mathbf{A}/c)^2-\mu_B\boldsymbol{\sigma}\cdot\mathbf{M}+V, \tag{1}$$

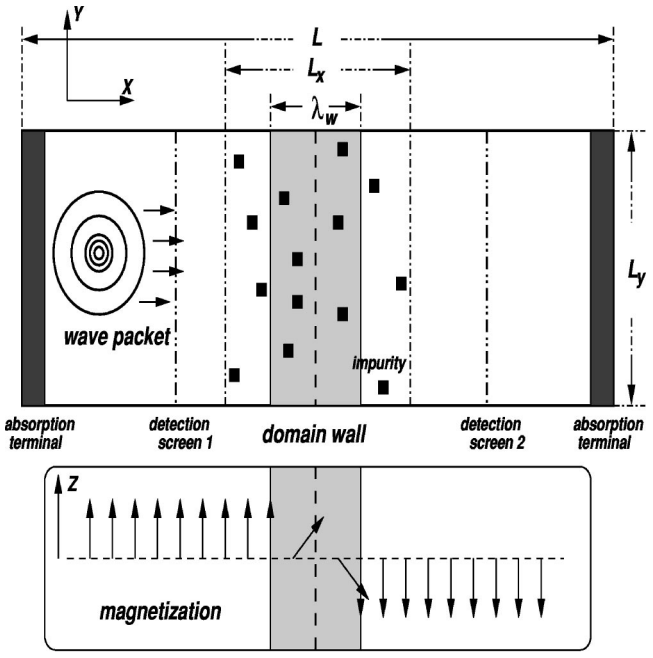

FIG. 1. The geometry of the simulation model of a mesoscopic metallic wire containing a magnetic domain wall of width λ_w. Black squares: Impurities distributed randomly over an area of size $L_x \times L_y$. The gray stripes at the edges indicate regions where electrons entering these regions are being absorbed. The detector screens 1 and 2 measure the electrical current through these screens. Also shown is a schematic diagram of the magnetization inside the strip.

where $\mathbf{p}=(p_x,p_y)$ is the momentum operator of the electron with effective mass m^*, $\boldsymbol{\sigma}=(\sigma^x,\sigma^y,\sigma^z)$ denote the Pauli spin matrices. $\mathbf{M}=\mathbf{M}(x,y)$ describes the magnetization in the material and $V=V(x,y)$ represents the potential due to nonmagnetic impurities. We neglect the vector potential $\mathbf{A}$ resulting from the sum of the atomic magnetic-dipole contributions because in the case of a thin wire, it has little effect on the electron transport.

Following,[7,13] we assume that the magnetic domain wall can be described by

$$M_x(x,y)=M_0\,\mathrm{sech}\left(\frac{x-x_0}{\lambda_w}\right) \tag{2}$$

and

$$M_z(x,y)=M_0\tanh\left(\frac{x-x_0}{\lambda_w}\right), \tag{3}$$

with x_0 the center of the domain wall and λ_w a measure of its extent. Note that $M_z^2(x,y)+M_x^2(x,y)=M_0^2$ so that at each point (x,y) the magnetization is constant. For a schematic picture of how the magnetization changes with x see Fig. 1.

For each impurity we take a square potential barrier, i.e.,

$$V_n(x,y)=\begin{cases}0, & (x,y)\notin S_n\\ V_0, & (x,y)\in S_n,\end{cases} \tag{4}$$

where S_n denotes a square with label n. The position of the square is drawn from a uniform random distribution, rescaled to an area of size $L_x\times L_y$ (see Fig. 1). The concentration of impurities, c is given by $c=\Sigma_{n=1}^{N}S_n/(L_xL_y)$ where N denotes the total number of impurities. The potential entering in Eq. (1) is given by $V=V(x,y)=\Sigma_{n=1}^{N}V_n(x,y)$.

We will follow two routes to study the effect of the domain wall on the electrical conductivity: (1) By solving the time-dependent Schrödinger equation (TDSE) and (2) through an extension of the Kubo-formula-based theory of Tatara and Fukuyama.[13] The results of these two fundamentally different approaches can be compared by making use of the Landauer formula[14,15] relating the conductivity σ to the tranmission coefficient T. Notice however that the analytical result, obtained by averaging over impurity configurations will be compared with numerical results for different realizations of impurity configurations.

In the TDSE approach the procedure to calculate the transmission coefficient T consists of three steps. First the incoming electrons are represented by a wave packet with average momentum $\langle\mathbf{p}\rangle=\hbar\mathbf{k}=(\hbar k_F,0)$. For concreteness we take this intitial state to represent electrons with spin up only, i.e.,

$$\begin{aligned}\Psi(x,y,t=0)&=[\psi_\uparrow(x,y,t=0),\psi_\downarrow(x,y,t=0)]\\&=(\psi_\uparrow(x,y,t=0),0),\end{aligned} \tag{5}$$

and $\int dxdy|\Psi(x,y,t=0)|^2=1$. This initial state mimics the presence of the infinitesimal electric field entering the derivation of the Kubo formula: We only consider the electrical current due to the electrons that move with an average momentum $\langle\mathbf{p}\rangle=(\hbar k_F,0)$. Alternatively, in the TDSE approach it is a simple matter to add to V a potential corresponding to an electric field in the x direction. As a check, we ran several of such simulations and found that the results are the same as long as the electric field is a perturbation.

The second step involves the solution of the TDSE

$$i\hbar\frac{\partial\Psi(x,y,t)}{\partial t}=\mathcal{H}\Psi(x,y,t) \tag{6}$$

for sufficiently long times. The method we use to solve the TDSE has been described at length elsewhere,[16,17] so we omit details here. As indicated in Fig. 1, we place imaginary detection screens at various x positions. The purpose of each screen is to record the accumulated current that passes through it (the wave function is not modified by this detection process). Dividing the transmitted current (detector 2, see Fig. 1) by the incident current (detector 1) yields the transmission coefficient T. As the simulation package[16,17] that we use solves the TDSE subjected to Dirichlet boundary conditions, some precautions have to be taken in order to suppress artifacts due to reflections from the boundaries at $x=0,x=L$. We have chosen to add to V, an imaginary linear potential that is non-zero near the edges of the sample, as indicated by the gray strips in Fig. 1, and found that the absorption of intensity that results is adequate for the present purpose.

For numerical work it is convenient to rewrite the TDSE (6) in a dimensionless form. Taking the Fermi wavelength λ_F as the characteristic length scale of the electrons, the energy is measured in units of the Fermi-energy $E_F=h^2/(2m\lambda_F^2)$ and time in units of $\hbar/E_F$. For our model simulations we have taken $L=100\,\lambda_F$, $L_y=6.5\,\lambda_F$, $\mu_BM_0=0.4\,E_F$, $V_0=100\,E_F$ and $S_n=0.25\,\lambda_F^2$.

In Figs. 2 and 3 we show some snapshots of the probability distribution for the spin-up (top) and spin-down (bottom) part of the electron wave, moving through an impurity-free region. Initially at $t=0$, the probability for having electrons with spin-down is zero. As the wave moves to the right, the M_x component of the magnetization causes the spin to rotate, resulting in a conversion of electrons with spin up into electrons with spin down. For realistic values of the strength (i.e., $\mu_BM_0<E_F$) and width of the domain wall (i.e., $\lambda_w>\lambda_F$) the conversion will be almost 100% (for all practical purposes), which leads to a negligibly small reflection.[7] We have chosen $\lambda_w=2\,\lambda_F,\ldots,16\,\lambda_F$, which may be reasonable in the case of a very narrow wire or a strong anisotropy.

In the presence of impurities two new effects appear:

1. As a result of the scattering by the potential barriers electrons will be reflected, leading to a reduction of the transmission coefficient in the sense of Boltzmann transport. At the same time interference among scattered electrons leads to weak localization, and this quantum-mechanical effect also suppresses the transmission. Obviously, these effects are present in the absence of a domain wall as well.

2. As a result of the presence of the domain wall, electrons that are backscattered *and* have their spin reversed due to the wall, no longer interfere with electrons whose spin is

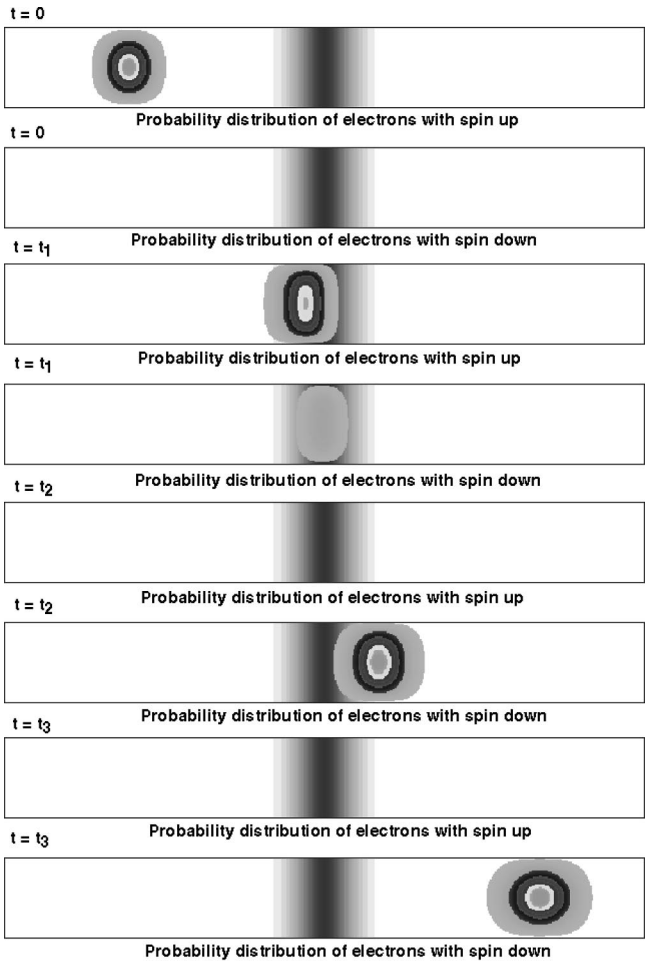

FIG. 2. Snapshots of the time evolution of the electron wave packet moving through an impurity free mesoscopic wire containing a domain wall with $\lambda_w = 2\lambda_F$ (represented by the smooth gray area), taken at $t_1 = 75\ \hbar/E_F$, $t_2 = 100\ \hbar/E_F$, and $t_3 = 150\ \hbar/E_F$.

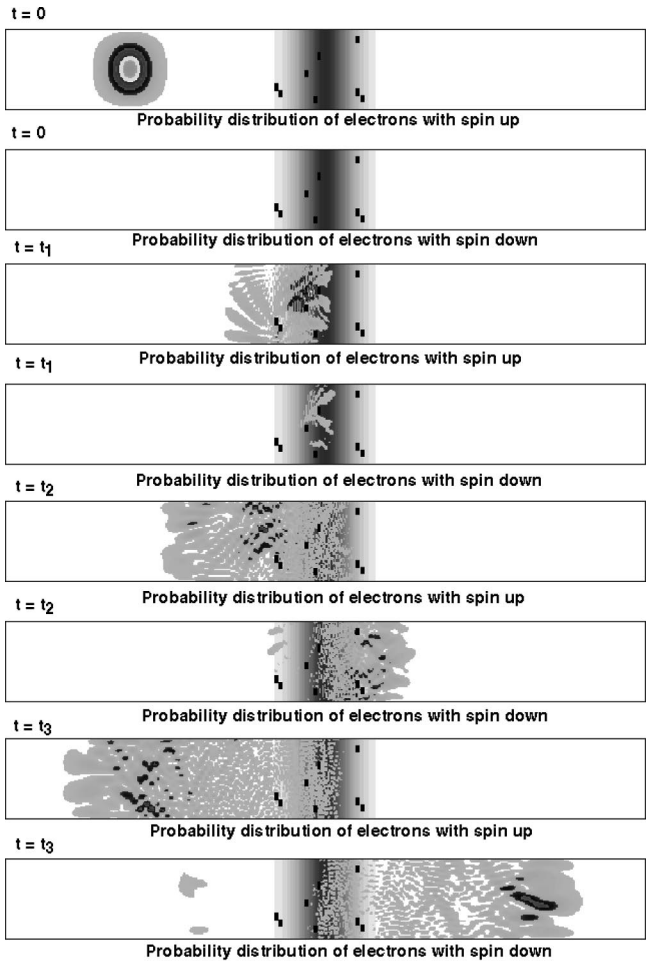

FIG. 3. Snapshots of the time evolution of the electron wave packet moving through a mesoscopic wire with impurities (represented by small black dots) with an impurity concentration $c = 2\%$ containing a domain wall ($\lambda_w = 2\lambda_F$), taken at $t_1 = 75\ \hbar/E_F$, $t_2 = 100\ \hbar/E_F$, and $t_3 = 150\ \hbar/E_F$.

unchanged. Hence, the effect of the domain wall is to reduce the enhanced backscattering due to the interference. On the basis of this argument it is to be expected that in the presence of a domain wall the transmission coefficient can be larger than in the absence of it.

In our simulations the contribution due to quantum interference effects resulting from the presence of the domain wall can be separated from all other contributions by a simple procedure: We compute the ratio of the transmission with (T) and without (T_0) a domain wall.

Some representative results of our calculations are depicted in Figs. 4–8. The simulation data shown are obtained from a single realization of the impurity distribution. No ensemble averaging of the transmission coefficient has been performed. The transmission in the absence of the wall (T_0) is plotted in Fig. 4 as a function of impurity concentration in the case of $L_x = 16$. In Figs. 5 and 6 we show the ratio T/T_0 as a function of the impurity concentration c, for $L_x = 8$ and $L_x = 16$, respectively. The two sets of simulation data in Fig. 5 correspond to different impurity configurations, and the difference between the two is due to a different interference pattern. The enhancement alluded to above is clearly present. The effect of conversion of the electron spin by the wall is amplified considerably by quantum interference at larger impurity concentration. The larger the scattering the more effective the domain wall is in converting electrons with spin up into electrons with spin-down.

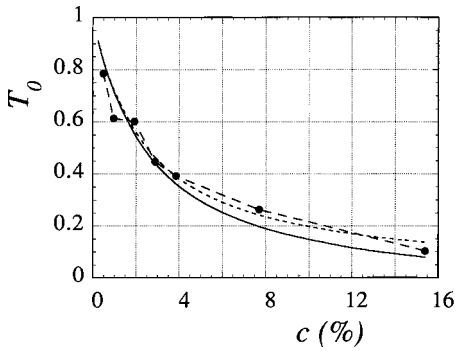

FIG. 4. Transmission in the absence of domain wall T_0 as a function of impurity concentration c for the case of $L_x = 8\ \lambda_F$. Solid and dotted line denotes the result of Kubo formula with and without the weak-localization correction taken into account, respectively. The effect of weak localization lowers the transmission at large c. Parameters are $\alpha = 0.05$ and $\beta = 6$ [see Eq. (8)].

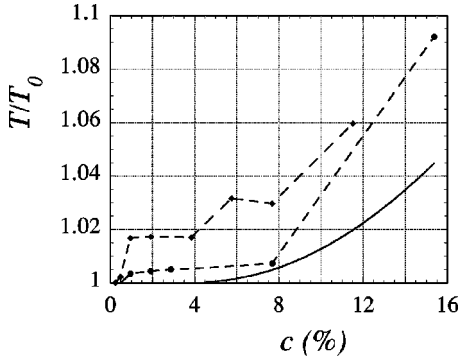

FIG. 5. Relative enhancement T/T_0 of the transmission resulting from the presence of the domain wall as a function of impurity concentration c. The width of the domain wall is $\lambda_w = 2\ \lambda_F$ and $L_x = 16\ \lambda_F$ (see Fig. 1). Simulation data for different impurity configurations are represented by diamonds and circles (the dashed and dotted line are guides to the eye only). Also shown is the theoretical result (10) with $\alpha = 0.05$ and $\beta = 6$ (solid line).

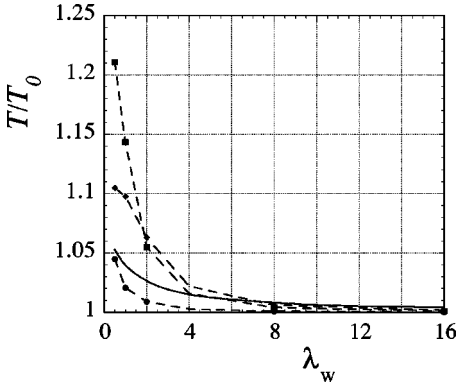

FIG. 7. Relative enhancement T/T_0 of the transmission as a function of the width λ_w of the domain wall for various impurity concentrations c and $L_x = 4\ \lambda_F$. The circles, squares, and diamonds correspond to $c = 3.85\%$, $c = 7.69\%$, and $c = 15.38\%$, respectively. The solid line depicts the theoretical result for $c = 15.38\%$ ($\alpha = 0.02$, $\beta = 6$).

In Figs. 7 and 8 we present results for domain walls of different width λ_w, keeping fixed the area in which the impurities are present ($L_x = 4$, and $L_x = 8$, respectively). The net result of increasing λ_w in this case is to reduce the effectiveness of the $M_x\sigma^x$ term in the Hamiltonian. Indeed by increasing λ_w, $M_x(x,y)$ becomes more smooth, hence less effective in the sense that less backscattered electrons flip their spin.

Let us compare these results with the analytical result based on Kubo formula, which is obtained by extending the theory of Tatara and Fukuyama.[13] In the absence of a domain wall the conductivity in two dimensions with the effect of weak localization taken into account is given by

$$\sigma_0 = \frac{e^2 n \tau}{m} - \frac{2e^2}{\pi\hbar}\frac{1}{V}\sum_q \frac{1}{q^2} = \frac{e^2}{h} n \lambda_F l \left(1 - \frac{\lambda_F}{l}\frac{2}{\pi^3}\frac{L_x}{L_y}\right), \tag{7}$$

where n is the electron density, τ and $l \equiv (\hbar k_F \tau/m)$ being the elastic lifetime and the mean free path, respectively. We have carried out the q-summation in one dimension, since L_y is much smaller than the inelastic diffusion length in the absence of the wall, which should be regarded as infinity in the simulation here. The transmission coefficient T_0 is related to the conductivity by $\sigma_0 = (e^2/h)(L_x/L_y)[T_0/(1 - T_0)]$ and thus

$$T_0 \simeq \frac{\beta}{\beta + \nu c}\left[1 - \frac{\nu c^2}{\beta + \nu c}\frac{2}{\pi^3}\frac{1}{\alpha}\frac{L_x}{L_y}\right], \tag{8}$$

where $\beta \equiv n\lambda_F^2 \alpha$, $\nu \equiv (L_x/L_y)$ and the mean free path is related to c through $l \equiv \alpha\lambda_F/c$. We treat α and β as fitting parameters. The solid curve in Fig. 4 is obtained for $\alpha = 0.05$ and $\beta = 6$ (or equivalently $l \sim 0.5\lambda_F \simeq 3k_F^{-1}$ for $c = 0.1\%$, which appears to be reasonable). The dotted line is the classical contribution to T_0 [i.e., the first term in Eq. (8)] and it is larger than T_0 at large c.

The perturbative treatment of the Kubo formula together with the averaging over impurity configurations leads to expressions [e.g., Eqs. (7) or (8)] that contain a relaxation time τ. Strictly speaking no such relaxation time is present in our

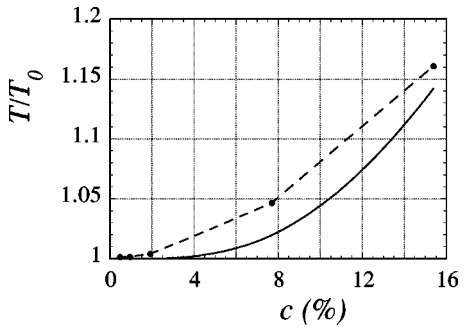

FIG. 6. Relative enhancement T/T_0 of the transmission resulting from the presence of the domain wall as a function of impurity concentration c. The width of the domain wall $\lambda_w = 2\ \lambda_F$ and $L_x = 8\ \lambda_F$ (see Fig. 1). Circles: simulation data; solid line: theoretical result (10) ($\alpha = 0.02$, $\beta = 6$).

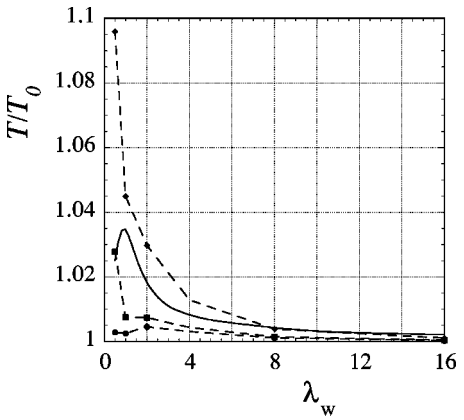

FIG. 8. Relative enhancement T/T_0 of the transmission as a function of the width λ_w of the domain wall for various impurity concentrations c and $L_x = 8\ \lambda_F$. The circles, squares, and diamonds correspond to $c = 3.85\%$, $c = 5.77\%$, and $c = 7.69\%$, respectively. The solid line depicts the theoretical result for $c = 7.69\%$ ($\alpha = 0.02$, $\beta = 6$).

TDSE calculations: There is only elastic scattering by impurities. In perturbation theory the main contribution to this scattering can be described in terms of an effective diffusive-scattering model characterized by τ. As shown in Fig. 4 this model works well for the case at hand.

In the presence of a domain wall the conductivity is expressed as

$$\sigma = \frac{e^2}{h} n l \lambda_F \left[1 - \frac{1}{2\pi^2} \frac{\lambda_F^2}{\lambda_w L} - \frac{2}{\pi^2} \frac{\lambda_F}{l} \left(\frac{L_w}{L_y} \tan^{-1} \frac{L_x}{\pi L_w} \right) \right], \tag{9}$$

where the second term is the classical contribution from the wall reflection and the third term is a weak localization correction with the effect of the wall included. The effect of the wall is to cause dephasing among the electron as is represented by the inelastic diffusion length, $L_w \equiv \sqrt{D\tau_w}$, $D \equiv \hbar^2 k_F^2 \tau / 2m^2$ being the diffusion coefficient. Here, τ_w is the inelastic lifetime due to the spin-flip scattering by the wall, $\tau_w^{-1} \equiv (\lambda_F E_F)^2 / (24\pi^2 \lambda_w L_x \Delta^2 \tau)$ ($\Delta \equiv \mu_B M_0$ denoting the Zeeman splitting).[13] The expression of T/T_0 is obtained as

$$\frac{T}{T_0} = 1 + \frac{\nu c^2}{\beta + \nu c} \frac{1}{\alpha} \left[\frac{2}{\pi^3} \frac{L_x}{L_y} \left(1 - \frac{\pi L_w}{L_x} \tan^{-1} \frac{L_x}{\pi L_w} \right) - \frac{1}{2\pi^2} \frac{\lambda_F^2}{\lambda_w L_x} \right]. \tag{10}$$

The result is plotted as solid lines in Figs. 5–8. The classical contribution (the last term) is negligibly small compared with the quantum correction in the region we are interested, and thus the enhancement of the transmission by the wall is seen. We have used the same value of parameter $\beta = 6$, but with different α ($\alpha = 0.05$ for Fig. 5 but $\alpha = 0.02$ for Figs. 6-8). We think this dependence of α on L_x is due to the ambiguity in relating the mean free path in Kubo formula to c in the simulation. Results of Eq. (10) thus obtained explain the simulation data well.

This work was partially supported by the ''Stichting Nationale Computer Faciliteiten (NCF),'' the NWO Priority Program on Massive Parallel Processing, and a Grant-in-Aid for Scientific Research from the Japanese Ministry of Education, Science and Culture. G.T. thanks the Alexander von Humboldt Foundation for financial support.

*Electronic address: jonkers@phys.rug.nl.
†Electronic address: deraedt@phys.rug.nl.
‡Electronic address: tatara@ess.sci.osaka-u.ac.jp.

[1] T.N. Todorov and G.A.D. Briggs, J. Phys.: Condens. Matter **6**, 2559 (1994).
[2] M. Viret, D. Vignoles, D. Cole, J.M.D. Coey, W. Allen, D.S. Daniel, and J.F. Gregg, Phys. Rev. B **53**, 8464 (1996).
[3] J.F. Gregg, W. Allen, K. Ounadjela, M. Viret, M. Hehn, S.M. Thompson, and J.M.D. Coey, Phys. Rev. Lett. **77**, 1580 (1996).
[4] U. Ruediger, J. Yu, S. Zhang, A.D. Kent, and S.S.P. Parkin, Phys. Rev. Lett. **80**, 5639 (1998).
[5] K. Hong and N. Giordano, J. Phys.: Condens. Matter **10**, L401 (1998).
[6] Otani *et al.* (unpublished).
[7] G.G. Cabrera and L.M. Falicov, Phys. Status Solidi B **61**, 539 (1974).
[8] P.M. Levy and S. Zhang, Phys. Rev. Lett. **79**, 5110 (1997).
[9] M.N. Baibich, J.M. Broto, A. Fert, F. Nguyen Van Dau, F. Petroff, P. Eitenne, G. Creuzet, A. Friederich, and J. Chazelas, Phys. Rev. Lett. **61**, 2472 (1988).
[10] G. Binach, P. Grunberg, F. Saurenbach, and W. Zinn, Phys. Rev. B **39**, 4828 (1989).
[11] J.J. Krebs, P. Lubitz, A. Chaiken, and G.A. Prinz, Phys. Rev. Lett. **63**, 1645 (1989).
[12] S.S.P. Parkin, N. More, and K.P. Roche, Phys. Rev. Lett. **64**, 2304 (1990).
[13] G. Tatara and H. Fukuyama, Phys. Rev. Lett. **78**, 3773 (1997).
[14] R. Landauer, J. Phys.: Condens. Matter **1**, 8099 (1989).
[15] S. Datta, in *Electronic Transport in Mesoscopic Systems* (Cambridge University Press, Cambridge, 1995).
[16] H. De Raedt and K. Michielsen, Comput. Phys. **8**, 600 (1994).
[17] H. De Raedt, in *Annual Reviews of Computational Physics IV*, edited by D. Stauffer (World Scientific, Singapore, 1996), p. 107.